ChemComm

COMMUNICATION

View Article Online
View Journal | View Issue

Cite this: *Chem. Commun.*, 2026, **62**, 5241

Received 18th December 2025,
Accepted 10th February 2026

DOI: 10.1039/d5cc07213a

rsc.li/chemcomm

Quantifying static capacity losses in solid-state battery composites *via* coulometric titration comparison

Kilian Vettori, †*[a] Maximilian Kissel, †[a] Daniel Wagner,[a] Steffen Schröder[b] and Jürgen Janek *[a]

An electrochemical method is discussed to quantify *in situ* the static CAM utilization, *i.e.*, the fraction of electrochemically active mass in solid-state battery composite cathodes. For that, coulometric titration curves of the same active material in cells with solid and liquid electrolytes are compared. The results are contrasted with an *ex situ* method based on X-ray diffraction.

Solid-state batteries (SSBs) have attracted substantial attention in recent years due to their potential to deliver higher energy and power density, along with expected improved safety compared to conventional lithium-ion batteries (LIBs) that use liquid electrolytes (LE).[1,2] Despite the potential benefits, several challenges must be overcome before SSBs can be widely commercialized.[3] This includes issues such as interfacial instability between the electrodes and the solid electrolyte (SE), as well as chemo-mechanical degradation, which currently limits performance and long-term stability.[4] While the goal for the negative side is a reservoir-free lithium metal electrode, the energy density of the cell is limited by the positive electrode, which is designed as a composite of cathode active material (CAM), SE and conductive additives.[5]

As a figure of merit, CAM-specific capacities and capacity losses are often calculated with respect to the mass of CAM in the cathode, $m_{\mathrm{CAM,tot}}$, and used to compare the performance of different composites or cells.[6] In a recent study, we discussed the importance of differentiating between static and kinetic capacity losses in SSB composite cathodes and revealed that different composite mixing can be a main reason for variations in mass-specific capacities with respect to $m_{\mathrm{CAM,tot}}$.[7] Thereby, a central challenge of SSB composites is to properly connect all CAM particles electronically. If this is not achieved, lower mass-specific capacities are observed in SSBs compared to LIBs. We recommend to consider these as static capacity losses.[7,8] The accurate evaluation of mass-specific capacities accounting for static capacity loss of SSBs is critical to avoid data misinterpretation at an early stage of research and for quality control during scale-up.

In the present work, we discuss a reliable and simple electrochemical method to estimate *in situ* the actual electrochemically active mass, $m_{\mathrm{CAM,act}}$, for a given SSB (half) cell with respect to a reference LIB measurement. The methodology is further called coulometric titration comparison (CTC) and has been successfully employed in several of our previous publications.[7–11] CTC shall be highlighted as well as critically discussed here in depth to be more easily implemented by other scientists testing active materials in different electrolyte systems. First, we sketch the differences between LIB and SSB cathode microstructures and their consequences for the capacities during cycling. Then, we illustrate the working principle and the experimental approach of CTC and discuss underlying assumptions as well as natural limitations of the method, including the numerical uncertainty of the method. Finally, we show the results of CTC from an exemplary measurement with $LiNi_{0.82}Mn_{0.07}Co_{0.11}O_2$ (NCM82) in an SSB composite cathode with Li_6PS_5Cl as the SE, and in a porous cathode in organic LE. The determined active mass $m_{\mathrm{CAM,act}}$ and the resulting CAM utilization $\Theta_{\mathrm{CAM,SSB}}$ are compared with Rietveld-refined *ex situ* XRD measurements on composite cathodes, revealing the fraction of electronically unconnected, inactive CAM.

Let us first picture the difference in connectivity of CAM particles in the cathodes of LIBs and SSBs (Fig. 1). In conventional LIBs a porous, electron-conducting network of CAM particles, binder, and carbon additives is infiltrated by LE.[12,13] In this porous electrode design, it can be assumed that nearly all CAM particles are ionically and electronically connected and thus electrochemically active (Fig. 1a). For discussion of this assumption the reader is referred to SI Section S2.1. Differences

[a] *Institute of Physical Chemistry & Center for Materials Research (ZfM/LaMa), Justus-Liebig-University Giessen, Heinrich-Buff-Ring 17, 35392, Giessen, Germany. E-mail: kilian.vettori@uni-giessen.de, juergen.janek@phys.chemie.uni-giessen.de*
[b] *Institute of Experimental Physics I & Center for Materials Research (ZfM/LaMa), Justus Liebig-University Giessen, Heinrich-Buff-Ring 16, 35392, Giessen, Germany*
† These authors contributed equally.

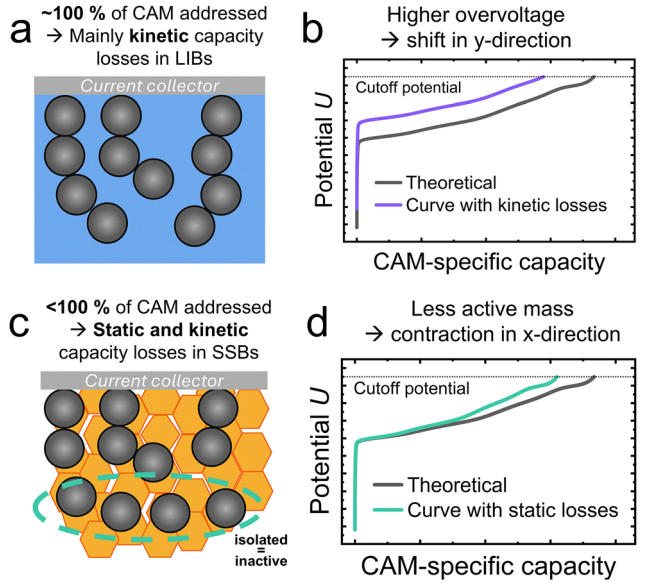

Fig. 1 Cathode designs in LIB and SSB. (a) In LIB, all CAM particles are assumed to be electrochemically active (validated in SI Section S2.1). (b) Thus, different CAM-specific capacities are the result of kinetic losses. (c) In SSB, electronic connection of CAM particles might be incomplete. (d) CAM-specific capacities of SSBs can be lower due to static capacity losses, in addition to kinetic losses. In practice, both processes are intertwined and lead to complex behaviour.

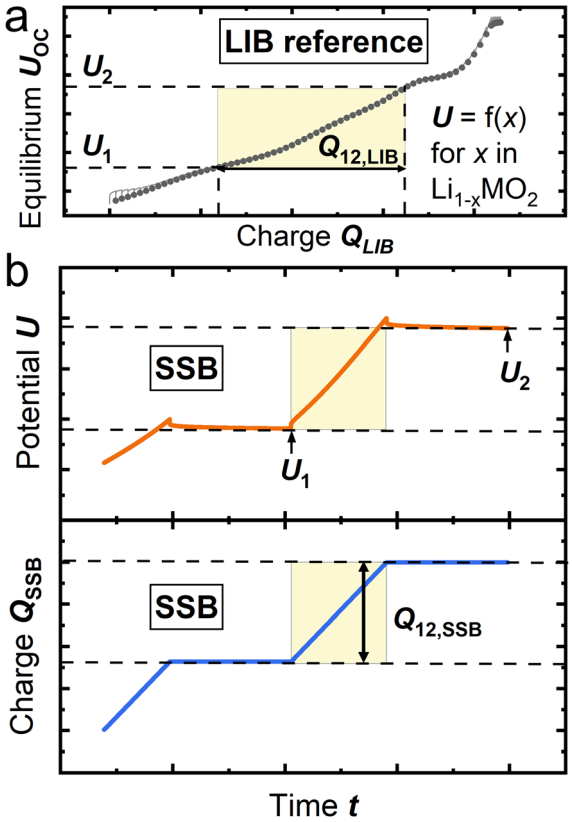

Fig. 2 Working principle of the CTC. (a) Coulometric titration data in LIB serving as reference, (b) potential and accumulated charge of SSB during charge and relaxation steps.

in measurable specific capacity q during the first cycles can then be mainly attributed to kinetic effects, which increase the overpotential (Fig. 1b), so that the cutoff potential is reached earlier.

The situation is different in composite cathodes in SSB cells (Fig. 1c). In this case, the CAM particles need to be mixed with a SE, which comprises particles with a specific size distribution, morphology, and mechanical properties that should be adapted to the properties of the CAM.[14,15] As shown in previous studies also by our group,[7,16] it can happen that a substantial amount of CAM particles is already from the beginning not incorporated in the electronic network, *e.g.* due to poor mixing. In both, LIB and SSB, carbon additives are used to electronically connect the CAM particles. For LIBs more porous carbons are used, whereas SSBs often employ carbon nanofibers (CNF) for long range connection.

The unconnected CAM particles do not take part in charging/discharging, and must be considered as electrochemically inactive, lowering $m_{CAM,act}$. Thus, in addition to kinetic capacity losses, substantial static capacity losses[7] need to be considered, which are visible by a horizontal compression of the charging curve (Fig. 1d). To accurately evaluate the specific capacity and avoid data misinterpretation, precise knowledge of the actual electrochemically active mass $m_{CAM,act}$ in SSB composite cathodes is required.[7]

Here, CTC represents a straightforward approach to quantify $m_{CAM,act}$ and $\Theta_{CAM,SSB}$. The corresponding procedure is sketched in Fig. 2 and will be elaborated in the following for NCM82. Experimental details are given in the SI Section S1.

First, a LIB cell is built as reference, and a coulometric titration curve, *e.g.* based on the galvanostatic intermittent titration technique (GITT),[17] is recorded (Fig. 2a). The open circuit potential (OCP) follows a characteristic function *vs.* the lithium content x in $Li_{1-x}NCMO_2$, which can also be expressed as state-of-charge (SoC) or mass specific capacity q.[18,19] These thermodynamic data serve as the reference curve. Coulometric titration measurements contain inherent errors which are discussed below and estimated in detail in SI Section S2.

To calculate $m_{CAM,act}$ in the SSB composite cathode, two equilibrated potentials U_1 and U_2, and the charge $Q_{12,SSB}$ that was accumulated to reach U_2 need to be known (Fig. 2b). $Q_{12,SSB}$ is then compared to the corresponding $Q_{12,LIB}$ from LIB data.

Together with $m_{CAM,LIB}$, *i.e.*, the total mass of CAM in the LIB cathode, the actual electrochemically active mass of the SSB cathode can be calculated with eqn (1):

$$m_{CAM,act} = m_{CAM,LIB}\frac{Q_{12,SSB}}{Q_{12,LIB}} \quad (1)$$

If less CAM is statically active, after reaching U_2 (or the corresponding SoC), the SSB has accumulated less charge $Q_{12,SSB}$ compared to the LIB. The fraction of active CAM in the SSB, *i.e.* the CAM utilization $\Theta_{CAM,SSB}$, can then be calculated *via* eqn (2):

$$\theta_{CAM,SSB} = m_{CAM,act}/m_{CAM,tot} \quad (2)$$

The following fundamental assumptions need to be considered when calculating the active mass *via* CTC:

First, it is assumed that in the LIB reference cell, 100% of the CAM is electrochemically active and thus all particles contribute to the coulometric titration curve (See SI Section S2.1). Furthermore, CAM utilization is understood as constant during the experiment.

Second, the potentials obtained for LIB and SSB need to be in equilibrium and follow the same titration curve of the pristine CAM. OCP values need to be in a region, where the titration curve is a well-defined and monotonically increasing function *vs.* the lithium content x.

Third, the capacity/charge measured is purely from de-/lithiation of the CAM, meaning a faradaic efficiency FE of 1 without contributions from other reactions, as *e.g.*, electrolyte decomposition.

Furthermore, to ensure a meaningful result for $m_{CAM,act}$, the parameters entering eqn (1) have to be carefully extracted, leading to the following experimental considerations:

The mass of CAM, which is used during the preparation of electrodes (LIB and SSB) is essential for a reliable application of CTC. This means that both $m_{CAM,tot}$ and $m_{CAM,LIB}$ enter the CAM utilization $\Theta_{CAM,SSB}$ with the weighing error. Furthermore, it is known that the CAM utilization in SSBs can be dynamic within the SoC, especially due to interparticle contact issues after volume contraction of NCM-type layered oxides above $\approx$4.2 V.[20] CTC is recommended at potentials where negligible chemo-mechanical changes in utilization occur in SSBs.[21,22]

The potentials need to be equilibrated. Thus, it is recommended to measure at potentials/SoCs where electrode kinetics is fast. For NCM, this is again at medium potentials/SoCs,[23–25] where diffusion of lithium is fast, allowing shorter relaxation times and avoiding concentration gradients.[26,27]

Obviously, SSB and LIB potentials need to be compared against the same reference potential. Since SSBs often employ other counter electrodes, their potentials need to be known and stable, as the In-InLi anode, with +620 mV *vs.* Li^+/Li (SI Section S3.1).[28]

Another consideration regards the OCP fading due to parasitic reactions, *e.g.* electrolyte decomposition re-lithiating the NCM. To quantify this, dU/dt at the end of relaxation, often called "OCV fading" or "self-discharge", at different potentials can be extracted and should be minimized experimentally.[29] The SI Section S2.3.1.2 shows such evaluation for the LIB reference cell. In general, it can be useful to use low loadings to reduce lithium concentration gradients in the cathode, coming with the cost of less precision for $m_{CAM,LIB}$. SI Section S2 provides data and recommendations on optimal experimental design. Potentials should be unique for a specific charge, meaning that two-phase regions/potential plateaus should be avoided, posing challenges for two-phase materials like $LiFePO_4$ (SI Section S2.2).[30] Finally the potential curve should be as close as possible to the pristine CAM, since extended processing is known to change the titration curve.[31]

The charge: We further recommend applying formation cycles to the cells to obtain stable titration curves for the active material, where the faradaic Efficiency (FE) of CAM de-/lithiation is close to 1 and no other processes like CEI formation are expected. Of course, cycling induced changes should be minimized. To identify voltage regions dominated by CAM de-/lithiation, we suggest comparing titration curves in both electrolytes.

We applied the CTC to two SSB cathode composite batches, which are expected to exhibit varying degrees of CAM utilization due to different electrode compositions.[16] One batch with a CAM:SE:CNF ratio of 70 : 30 : 1 (further called "good SSB" and shown in blue) and one with CAM:SE of 60 : 40 ("bad SSB", shown in orange).

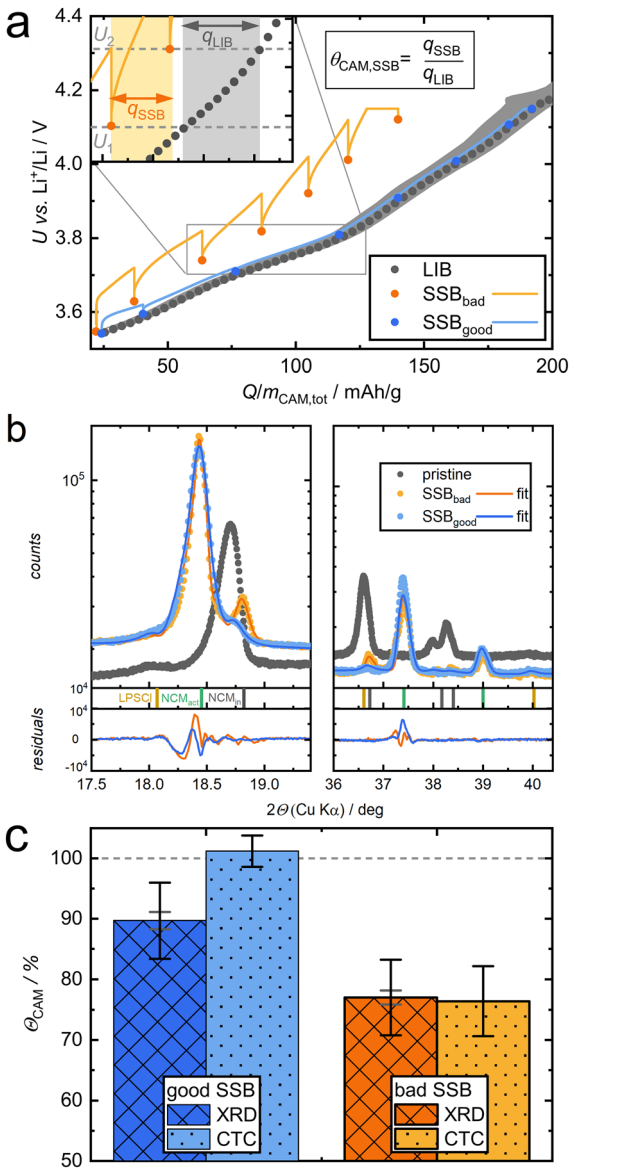

Fig. 3 Experimental results on good and bad SSB cathode composites. (a) Electrochemical data during application of CTC with LIB reference. The inlet shows an exemplary calculation of $\Theta_{CAM,SSB}$ for two OCPs of the bad SSB. (b) XRD spectra and Rietveld refinements with indicated reflex positions. (c) Resulting CAM utilization (eqn (2)) from XRD and CTC method. Grey error bars for XRD are from Rietveld refinement and black from an estimated error of 5 wt% per phase. Error bars for CTC are from application to multiple potential steps (SI Section S3.2).

We obtained multiple relaxed potentials for both SSBs by repeating a simple charge and relaxation protocol, shown by highlighted points in Fig. 3a. The SSB charge procedures (orange, blue data points) deviate from the coulometric titration data of the LIB reference (grey). The inlet showcases how a CAM utilization is calculated for two OCP values of the ''bad'' SSB. This procedure (eqn (2)) was applied for all neighboring OCPs and both cells as shown in SI Section S3.2 *via* a Python script.[32] From the obtained CAM utilizations we calculated a selected average (SI section S3.2), resulting in $\Theta_{CAM,SSB}$ of 76.4 ± 5.8% and 101.2 ± 2.6% for bad and good SSB, respectively.

Additionally, we performed XRD on the ''good'' and ''bad'' SSB composites after extracting them in the U_2 state after holding U = 4.15 V for 12 h. While the major part of the signal corresponds to active, delithiated NCM (NCM_{act}, green indicator) in H2 phase, distinct reflexes of inactive NCM (NCM_{inact}, grey indicator) in H1 phase are observed for both SSBs (Fig. 3b).[33] For comparison, also a pristine composite, containing only NCM_{inact}, is shown in grey. Full diffractograms are given in SI section S4. Shifting of reflexes due to changes in lattice parameters is well understood for NCM and can be compared for the used NCM82 with an *in situ* XRD in a liquid cell reference (SI Section S4). Following the approach by Bartsch *et al.*[34] and Strauss *et al.*[35] the XRD data were refined by the Rietveld method with two NCM phases and the SE phase, allowing an estimation of $\Theta_{CAM,SSB}$. The results of both methods, CTC and XRD, are compared in Fig. 3c. The XRD data validate the CTC method, delivering 89.7% CAM utilization for the good SSB in contrast to only 77.0% for the bad SSB. In SI Section S5 the charge curves of good and bad SSB are compared when being normalized to $m_{CAM,act}$ instead of $m_{CAM,tot}$.

We observe a systematically lower CAM utilization when quantified by XRD for SSBs that perform very well (as measured by CTC). This could be due to a LIB reference that suffers from similar capacity losses as the SSBs, thus overestimating $\Theta_{CAM,SSB}$. Another reason could be LPSCl contributing to capacity while the actual $m_{CAM,act}$ is lower. Most plausible is that Rietveld refinement of a phase with a minor volume fraction and correspondingly small signal in XRD data inherently leads to error-prone results, *e.g.* overinterpretation of device-related shoulders of reflexes.

We believe CTC offers multiple advantages over the approach based on XRD while allowing comparable accuracy. First, it requires no additional equipment and enables an *in situ* determination of $m_{CAM,act}$ instead of *ex situ* and *post mortem* measurements, which is typically done for XRD on SSBs. Furthermore, XRD data refinement as quantification of small mass fractions is inherently inaccurate.

In contrast, coulometric titration comparison (CTC) allows reliable *in situ* access to $m_{CAM,act}$. The procedure is simple to implement and allows an estimation of errors, providing a useful tool. We have applied it successfully to SSB composite cathodes and verified the results with an *ex situ* XRD method, but the procedure can be used for any suitable active material under the assumptions discussed in this work. Furthermore, best-practice is described regarding experimental design and the evaluation *via* Python script facilitates the implementation of CTC. In general, coulometric titration has proven to be highly useful within our working group as multiple publications employing CTC show.[7–11] Applied to SSBs, the possibility to uncover the presence of electrochemically inactive electrode material, may help to develop and optimize advanced cathode composites for next-generation applications.

Author contributions

Kilian Vettori: investigation, writing – original draft, software. Maximilian Kissel: investigation, writing – original draft. Daniel Wagner: formal analysis (XRD Rietveld refinements). Steffen Schröder: writing – review & editing. Jürgen Janek: supervision, writing – review & editing.

Conflicts of interest

There are no conflicts to declare.

Data availability

Coulometric titration data and measurements and the Python code used for evaluation are available in the CTC-data-analysis repository at https://doi.org/10.5281/zenodo.17967963.

Supplementary information (SI) is available. See DOI: https://doi.org/10.1039/d5cc07213a.

Acknowledgements

This work has been funded by the Federal Ministry of Research, Technology and Space under the project HIPOBAT (FKZ: 03XP0611E) and by Deutsche Forschungsgemeinschaft (DFG, German Research Foundation) through the Priority Program 2289 (Project 462470125).

References

1 A. M. Bates, Y. Preger, L. Torres-Castro, K. L. Harrison, S. J. Harris and J. Hewson, *Joule*, 2022, **6**, 742–755.
2 J. Janek and W. G. Zeier, *Nat. Energy*, 2016, **1**, 16141.
3 J. Janek and W. G. Zeier, *Nat. Energy*, 2023, **8**, 230–240.
4 A. Banerjee, X. Wang, C. Fang, E. A. Wu and Y. S. Meng, *Chem. Rev.*, 2020, **120**, 6878–6933.
5 S. Randau, D. A. Weber, O. Kötz, R. Koerver, P. Braun, A. Weber, E. Ivers-Tiffée, T. Adermann, J. Kulisch, W. G. Zeier, F. H. Richter and J. Janek, *Nat. Energy*, 2020, **5**, 259–270.
6 S. Puls, E. Nazmutdinova, F. Kalyk, H. M. Woolley, J. F. Thomsen, Z. Cheng, A. Fauchier-Magnan, A. Gautam, M. Gockeln, S.-Y. Ham, M. T. Hasan, M.-G. Jeong, D. Hiraoka, J. S. Kim, T. Kutsch, B. Lelotte, P. Minnmann, V. Miß, K. Motohashi, D. L. Nelson, F. Ooms, F. Piccolo, C. Plank, M. Rosner, S. E. Sandoval, E. Schlautmann, R. Schuster, D. Spencer-Jolly, Y. Sun, B. S. Vishnugopi, R. Zhang, H. Zheng, P. Adelhelm, T. Brezesinski, P. G. Bruce, M. Danzer, M. El Kazzi, H. Gasteiger, K. B. Hatzell, A. Hayashi, F. Hippauf, J. Janek, Y. S. Jung, M. T. McDowell, Y. S. Meng, P. P. Mukherjee, S. Ohno, B. Roling, A. Sakuda, J. Schwenzel, X. Sun, C. Villevieille, M. Wagemaker, W. G. Zeier and N. M. Vargas-Barbosa, *Nat. Energy*, 2024, **9**, 1310–1320.

7 M. Kissel, M. Schosland, J. Töws, D. Kalita, Y. Schneider, J. Kessler-Kühn, S. Schröder, J. Schubert, F. Frankenberg, A. Kwade, A. Bielefeld, F. H. Richter and J. Janek, *Adv. Energy Mater.*, 2025, **15**, 2405405.
8 G. Conforto, R. Ruess, D. Schröder, E. Trevisanello, R. Fantin, F. H. Richter and J. Janek, *J. Electrochem. Soc.*, 2021, **168**, 70546.
9 P. Minnmann, J. Schubert, S. Kremer, R. Rekers, S. Burkhardt, R. Ruess, A. Bielefeld, F. H. Richter and J. Janek, *J. Electrochem. Soc.*, 2024, **171**, 60514.
10 B.-X. Shi, Y. Yusim, S. Sen, T. Demuth, R. Ruess, K. Volz, A. Henss and F. H. Richter, *Adv. Energy Mater.*, 2023, **13**, 2300310.
11 B.-X. Shi, F. Weber, Y. Yusim, T. Demuth, K. Vettori, A. Münchinger, G. Titvinidze, K. Volz, A. Henss, R. Berger and F. H. Richter, *J. Mater. Chem. A*, 2025, **13**, 2600–2614.
12 A. Kwade, W. Haselrieder, R. Leithoff, A. Modlinger, F. Dietrich and K. Droeder, *Nat. Energy*, 2018, **3**, 290–300.
13 A. Shodiev, F. M. Zanotto, J. Yu, M. Chouchane, J. Li and A. A. Franco, *Energy Storage Mater.*, 2022, **49**, 268–277.
14 P. Minnmann, F. Strauss, A. Bielefeld, R. Ruess, P. Adelhelm, S. Burkhardt, S. L. Dreyer, E. Trevisanello, H. Ehrenberg, T. Brezesinski, F. H. Richter and J. Janek, *Adv. Energy Mater.*, 2022, **12**, 2201425.
15 A. Bielefeld, D. A. Weber and J. Janek, *ACS Appl. Mater. Interfaces*, 2020, **12**, 12821–12833.
16 A. Bielefeld, D. A. Weber and J. Janek, *J. Phys. Chem. C*, 2019, **123**, 1626–1634.
17 W. Weppner and R. A. Huggins, *J. Electrochem. Soc.*, 1977, **124**, 1569–1578.
18 M. Levi and D. Aurbach, *Electrochim. Acta*, 1999, **45**, 167–185.
19 M. D. Radin, S. Hy, M. Sina, C. Fang, H. Liu, J. Vinckeviciute, M. Zhang, M. S. Whittingham, Y. S. Meng and A. van der Ven, *Adv. Energy Mater.*, 2017, **7**, 1602888.
20 R. Koerver, W. Zhang, L. de Biasi, S. Schweidler, A. O. Kondrakov, S. Kolling, T. Brezesinski, P. Hartmann, W. G. Zeier and J. Janek, *Energy Environ. Sci.*, 2018, **11**, 2142–2158.
21 X. Liu, B. Zheng, J. Zhao, W. Zhao, Z. Liang, Y. Su, C. Xie, K. Zhou, Y. Xiang, J. Zhu, H. Wang, G. Zhong, Z. Gong, J. Huang and Y. Yang, *Adv. Energy Mater.*, 2021, **11**, 2003583.
22 S. H. Park, K. G. Naik, B. S. Vishnugopi, X. Xiao, M. Drakopoulos, N. T. Vo, Z. Zhong, P. P. Mukherjee and K. B. Hatzell, *ACS Nano*, 2025, 22262–22269.
23 A. Liu, N. Phattharasupakun, M. M. E. Cormier, E. Zsoldos, N. Zhang, E. Lyle, P. Arab, M. Sawangphruk and J. R. Dahn, *J. Electrochem. Soc.*, 2021, **168**, 70503.
24 R. Weber, A. J. Louli, K. P. Plucknett and J. R. Dahn, *J. Electrochem. Soc.*, 2019, **166**, A1779–A1784.
25 R. Morasch, H. A. Gasteiger and B. Suthar, *J. Electrochem. Soc.*, 2023, **170**, 80522.
26 M. D. Levi, K. Gamolsky, D. Aurbach, U. Heider and R. Oesten, *J. Electroanal. Chem.*, 1999, **477**, 32–40.
27 K. Vettori, S. Schröder, L. Ahrens, R. Wilhelm, S. Kremer, J. K. Eckhardt, T. Brezesinski, A. Kondrakov, J. Mayer, A. Henss and J. Janek, *Adv. Energy Mater.*, 2025, 2502148.
28 A. L. Santhosha, L. Medenbach, J. R. Buchheim and P. Adelhelm, *Batteries Supercaps*, 2019, **2**, 524–529.
29 T. Roth, L. Streck, A. Graule, P. Niehoff and A. Jossen, *J. Electrochem. Soc.*, 2023, **170**, 20502.
30 D. Di Lecce and J. Hassoun, *J. Phys. Chem. C*, 2015, **119**, 20855–20863.
31 L. Zheng, C. Wei, M. D. L. Garayt, J. MacInnis and M. N. Obrovac, *J. Electrochem. Soc.*, 2019, **166**, A2924–A2927.
32 K. Vettori, CTC-data-analysis, 2026, Zenodo10.5281/zenodo.17967963.
33 C. Ghanty, B. Markovsky, E. M. Erickson, M. Talianker, O. Haik, Y. Tal-Yossef, A. Mor, D. Aurbach, J. Lampert, A. Volkov, J.-Y. Shin, A. Garsuch, F. F. Chesneau and C. Erk, *ChemElectroChem*, 2015, **2**, 1479–1486.
34 T. Bartsch, A.-Y. Kim, F. Strauss, L. de Biasi, J. H. Teo, J. Janek, P. Hartmann and T. Brezesinski, *Chem. Commun.*, 2019, **55**, 11223–11226.
35 F. Strauss, T. Bartsch, L. de Biasi, A.-Y. Kim, J. Janek, P. Hartmann and T. Brezesinski, *ACS Energy Lett.*, 2018, **3**, 992–996.